Kapal: Jurnal Ilmu Pengetahuan dan Teknologi Kelautan
(Kapal: Journal of Marine Science and Technology)

2301-9069 (e)
1829-8370 (p)

journal homepage : http://ejournal.undip.ac.id/index.php/kapal

Study of Towing Lug Strength in 300 feet Barge at Docking Process

Andi Mursid Nugraha Arifudin[1)], Amalia Ika Wulandari[1)], Mohammad Ardha Wiku Wicaksono[1)]

[1)]Department of Naval Architecture, Institut Teknologi Kalimantan, Balikpapan 76127, Indonesia
[*)]Corresponding Author : andi.mursid@lecturer.itk.ac.id

Article Info

Keywords:
Towing Lug;
Pull Angel;
FEM;
Deformation;
Stress;

Article history:
Received: 02/02/2023
Last revised: 28/04/2023
Accepted: 29/04/2023
Available online: 29/04/2023
Published: 17/05/2023

DOI:
https://doi.org/10.14710/kapal.v20i2.52624

Abstract

Currently, the docking of ships or barges has been dominated by the airbag system by relying on the pull of the winch. For the Kalimantan area, the barge is generally pulled using a winch during docking. The structures that play a role when pulling the barge are towing brackets, slings, pulleys, and winches. In this paper, the towing lug will be the object of special discussion regarding its structural strength performance. The towing Lug model used when towing is in the form of an asymmetrical lobe. Two towing brackets are placed on the left and right sides of the bow barge. This towing lug sometimes damaged during towing, so it is necessary to simulate the strength of the towing lug using the finite element method (FEM). A 300 feet Barge is simulated with a total weight (W) of 1200 Tons. The towing lug design structure is made with 3 kinds of models with a varying number of layers and plate thickness. The towing lug design sample used in the existing shipyard is called model 1. While the other modifications to the 2 towing lug structures are called model 2 and model 3. Towing brackets are simulated using a computer with the help of Ansys software. The towing bracket's tensile angle is also varied to obtain a more attractive strength value. The variations of the pull angles used in this simulation are 80°, 83°, 85°, 87° and 90°. From the simulation results, it is obtained that the deformation values in each model show an insignificant level of change. In general, the simulation results also show stress values for each variation that tend to be safe and can be applied when the barge is towed to the dry dock. All equivalent stress values in each condition are still below the material yield stress. However, among the various simulations there are 2 types of conditions that experience stress values that exceed the class allowable stress.

1. Introduction

Docking a ship or barge on land is an activity that is often carried out at least twice during the validity period of the ship/barge certification to facilitate inspection. These inspections consist of a thorough operation that requires the assets to be towed to a special facility called a dry dock [1]. The aim is to carry out a technical evaluation of the hull condition after operation. With the hope that these improvements can maintain the same structure as when it was built and offered several services [2]. In general, ships and barges are pulled ashore during intermediate surveys and special surveys. Sometimes ships or barges are also brought ashore in emergencies. For shipyards like in the Kalimantan area today, the docking system used is the airbag system as shown in Figure 1. The simple operation causes the airbag system to be widely used in that area. In addition, the dry dock system using airbags meets technical feasibility and economic feasibility. So it can be concluded that the investment costs are relatively cheap when compared to other docking systems where savings can reach 40% [2]. To support docking activities using an airbag system, several supporting equipment must be prepared such as balloons, winches, pulleys, slings, chains, pond ropes, and towing brackets. All of these equipment have an important role in maintaining docking activities to avoid the occurrence of failure in pulling or launching.

Figure 1. Airbag application on docking Barge

One of the most important supporting structures to review is the towing lug as shown in Figure 2. The towing lug consists of a main plate and a pad eye which functions as a place to attach the chain to the barge that will be towed ashore. The structure of the towing lug will be simulated in this study using a numerical experiment that adopts the finite element method (FEM). Using the help of Ansys software, simple modeling with a 300 feet barge as the input load. Data on the size and shape of the towing brackets were obtained from a shipyard in East Kalimantan. This towing lug installed on the left and right sides of the bow barge. Incorrect installation and dimensioning of the towing lug structure usually causes barge towing and launching failure.

Figure 2. Towing lug on Barge

FEM is used as a case-solving method in this paper because FEM is a numerical method that is widely used to solve mechanical problems or to determine approximate solutions for a large class of engineering problems [3][4]. Generally, FEM is used for structural analysis and as a basis for verifying adequate load-bearing capacity such as beam or slab structures [5]. Analysis related to pad eye structural strength like this has been carried out by various researchers. Heo et al [6] tried to compare 2 types of lifting lugs between type D and type T with varying lifting angle arcs. The results of his research show that the T-type lug is better than the D-type. This research was conducted using a numerical method approach. In another study, Lee et al [7] presented to optimize the T-type lug thickness design using non-linear strength analysis. The results showed that there was a decrease in lug performance after experiencing a decrease in thickness for each lug capacity variation [5]. Furthermore, Lee et al [8] conducted a study regarding the effect of the direction of lift on the limit strength of the T-type lug. The results showed that the normal direction of the lug produces worse values if the direction of the force is tilted. Liu et al [9], conducted a study related to the issue of lifting eye pads by optimizing their thickness using FEA. The results of eye-bearing size optimization revealed a 50% saving in steel costs. Arifuddin et al [10], simulated the placement of a lifting pad eye to obtain the most optimal position using the stiffness method. The results of the study revealed that the location of the pad eye greatly influences the bending stress and deformation of the ship block. Antalffy et al [11], addressed the effect of vertical and horizontal lift angles on the tank pipe structure on ships. The analysis was carried out on the lug structure installed in the tank using FEM. The results of the study show a greater structural response in the horizontal direction. Lv et al [12], assessed a crack failure analysis on the backing plate on the lifting lug using the Finite Element Method. The results reveal that a high lift angle affects the von Mises stress.

The purpose of this study is to determine the response of the towing lug structure when pulling the barge ashore using airbags. The towing simulation is carried out by varying the barge pulling angle. In addition, the pad eye structure on the towing Lug varied to see the optimal pad eye layer arrangement. The structural responses considered in this study are normal stress, shear stress, and von mises stress. Furthermore, the deformation for each simulation will be investigated.

2. Methods

For all research problems in this paper are solved using software that adopts the finite element method (FEM). The research object will be modeled with a computer and then given structural treatment according to the conditions in the shipyard. Towing Lug simulated with a variety of pulling angles. The towing angle is modeled with 5 variations, namely 80^0, 83^0, 85^0, 87^0, and 90^0 as shown in Figure 3. For the towing Lugload that works it is assumed to pull a 300 feet barge, namely 1200 tons with the main size of the barge as shown in Table 1.

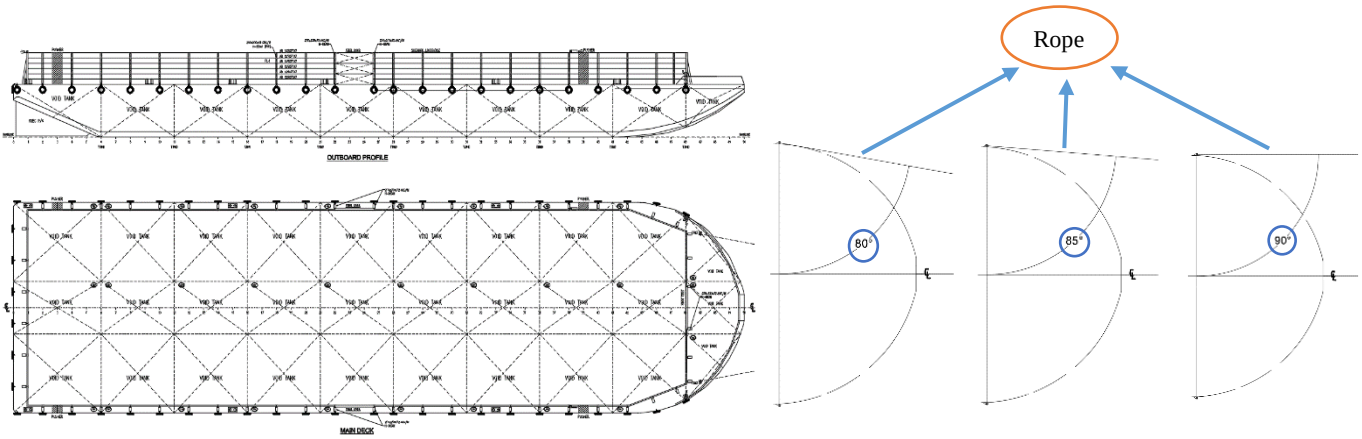

Figure 3. Barge and angle pull variations

Table 1. Main dimension of barge

Length Overall (L_{OA})	91,44 m
Breadth Moulded (B)	24,39 m
Depth Mouled (H)	6,10 m
Draft (T)	5,20 m
Light Wight Tonnage (LWT)	1296,00 Ton

The number of plate layers is also modified in the towing Lugas shown in Figure 4. The input load is the same for each variation. Furthermore, the structural response in the form of deformation and maximum stress will be identified for each variation. Meanwhile, the specifications for the material used are shown in Table 2.

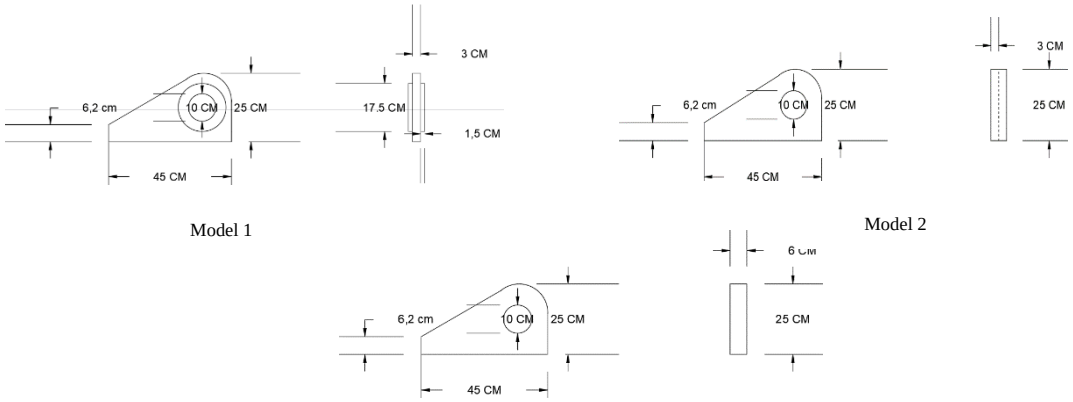

Figure 4. Padeye arrangement

Table 2. Material properties of A36-HT Steel [13]

Yield Stress	355 N/mm^2
Tensile Strength	630 N/mm^2
Elastic Modulus	2,1 x 10^5 N/mm^2
Density	7850 N/mm^3
Poisson Ratio	0,3

For the initial step, modeling was carried out using Ansys according to the towing Lugdimensions obtained from the Shipyard. The towing Lugmodel consists of the main plate and pad eye by adjusting the material specifications used in the Barge. In field conditions, two towing brackets are installed on the PS and SB sides of the bow of the barge, so it is assumed that the total weight acting on the towing Lug equal to the total weight divided by two. For the force equation acting on the towing lug when pulling the barge, use the following equation [14].

$$F = W\ (\mu\ cos\ \alpha + sin\ \alpha) \quad (1)$$

where ;

F = The pulling force generated by the sling system (ton)
W = Load (ton)

μ = Coefficient of rolling friction between the airbags and the runway 0,035 (concrete base)
α = The slope angle of the rampway ($2{,}3^{o} - 2{,}6^{o}$)

The bondary conditions applied in this simulation are for the translation direction Ux = 0, Uy = 0 and Uz = 0. The same application for the direction of rotation Rx = 0, Ry = 0 and Rz = 0. This bondary condition is applied with the assumption that the main plate is installed with perfect weld penetration like Figure 5. To evaluate the structural response that occurs, a comparison is then made with the allowable stress of Biro Klasifikasi Indonesia standart [15] with the following equation :

Normal Stress :

$$\sigma_N \leq \frac{150}{k} [N/mm^2] \quad (2)$$

Shear Stress :

$$\tau \leq \frac{100}{k} [N/mm^2] \quad (3)$$

Von Mises Stress :

$$\sigma_V = \sqrt{\sigma_N^2 + 3\tau^2} \leq \frac{180}{k} [N/mm^2] \quad (4)$$

Where ;

σ_N = Normal Stress (N/mm²)
τ = Shear Stress (N/mm²)
σ_V = Von Misses Stress (N/mm²)
k = Material Factor

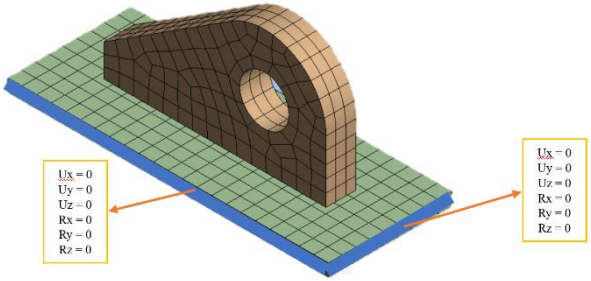

Figure 5. Boundary condition on towing lug model

3. Results and Discussion

3.1 Normal Stress

Simulations on models 1, 2, and 3 have been successfully carried out using numerical simulations as shown in Figure 5. Difference of the three structures on towing lug model is the thickness and pad eye layers arrangement. The pad eye on model 1 consists of 1 plate and is equipped with a ring-shaped doubling plate. Pad eye Model 2 consists of 2 plates joined to the same thickness without ring-shaped doubling plates. Whereas the pad eye model 3 only consists of 1 plate without doubling plates. The structures observed are structural performance phenomena on the main plate and pad eye. The minimum normal stress in model 1 is obtained at an angle of 80^0. Meanwhile, the maximum normal stress value in model 1 is obtained at an angle of 90^0. The average percentage increase in stress for each change in the angle of model 1 is 4.03%. Furthermore, for model 2, the minimum normal stress occurs at a pull angle of 80^0 and the maximum normal stress occurs at a pull angle of 90^0. The average percentage increase in stress for each angle change in model 2 is 3.58%. The same phenomenon also occurs in model 3, where the minimum normal stress value occurs at the pull angle of 80^0 and the maximum normal stress occurs at the pull angle of 90^0. The average percentage increase in stress for each angle change in model 3 is 3.53%. The distribution of normal stress values for each model can be seen in Table 3.

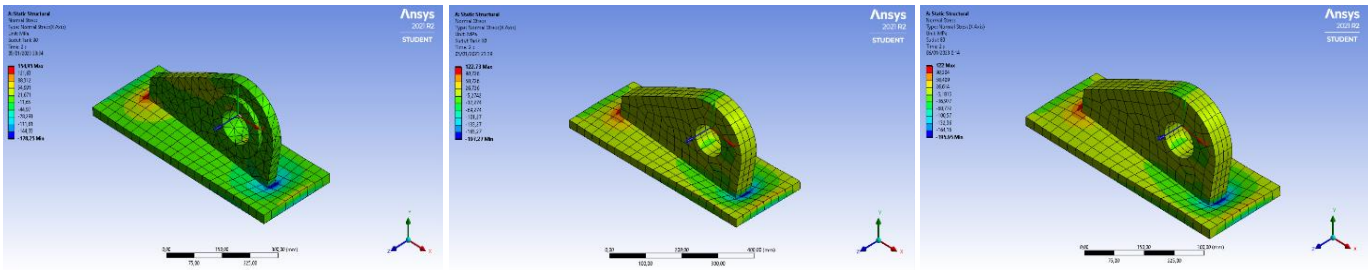

Model 1 Model 2 Model 3

Figure 5. Phenomenon of normal stress gradation on models with pull angle of 80^0

Table 3. normal stress on each towing lug models.

No.	Pull Angle Variations (º)	σ_N (N/mm²)			$\sigma_{allowable}$ (N/mm²)	$(\sigma_N) < (\sigma_{allowable})$		
		Model 1	Model 2	Model 3		Model 1	Model 2	Model 3
1	80	132.33	122.73	122.00	208.33	pass	pass	pass
2	83	140.13	129.28	128.43	208.33	pass	pass	pass
3	85	144.88	133.20	132.28	208.33	pass	pass	pass
4	87	149.24	136.73	135.74	208.33	pass	pass	pass
5	90	154.95	141.22	140.14	208.33	pass	pass	pass

The normal stress that occurs is then evaluated with the BKI class permit normal stress. Where, from the 3 simulated models, all stress values meet the class criteria. The description of the comparison of the stress values for each model can be seen in the graph in Figure 6. In general, from a normal stress perspective, all models and angle variations can be applied to the barge. However, it still needs to be considered on other types of working stress. The increase in normal stress on the three models shows the same trend. Model 1 seems to have a higher stress value than the other two models. This happens because the cross-sectional area of model 1 is smaller when compared to the cross-sectional area of models 2 and 3. The asymmetrical shape of the pad eye also affects the amount of stress for each pull angle. The cross-section of the structure at the pad eye also changes when the direction of the force is also changed. The cross section of the eye is getting smaller from 80^0 to 90^0.

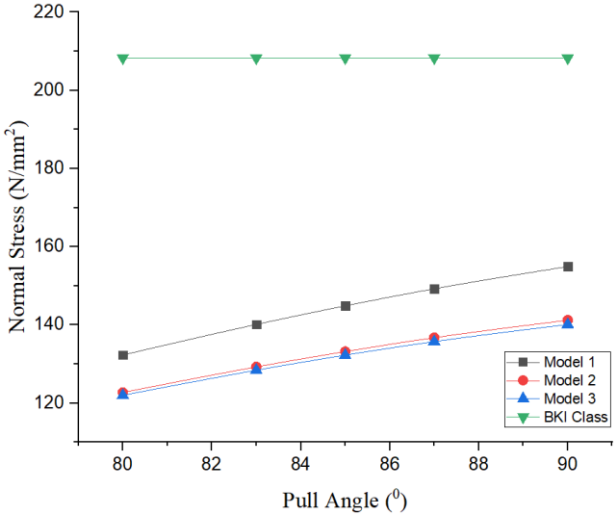

Figure 6. Normal stress distribution on towing lug models

3.2 Shear Stress

The results of the shear stress test on the towing Lughave been carried out in models 1, 2, and 3 as shown in Figure 7. The minimum shear stress in model 1 is obtained at a pull angle of 90^0. Meanwhile, the maximum shear stress value in model 1 is obtained at a pull angle of 80^0. the average percentage of the stress drop for each change in the angle of model 1 is -9.18%. Furthermore, for model 2, the minimum shear stress occurs at a pull angle of 90^0 and the maximum shear stress occurs at an angle of 80^0. The average percentage value of the stress drop for each change in the angle of model 2 is -8.04%. The same phenomenon also occurs in model 3, where the minimum shear stress occurs at a pull angle of 90^0 and the maximum shear stress occurs at an angle of 80^0. The average percentage increase in stress for each angle change in model 3 is -8.74%. The distribution of shear stress values for each model can be seen in Table 4.

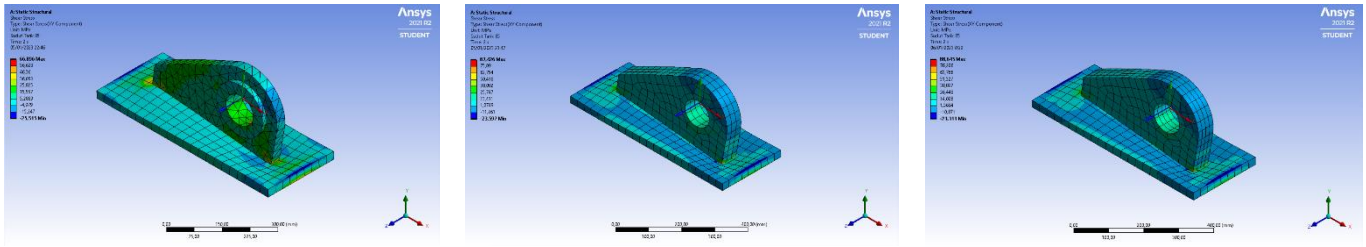

Model 1 Model 2 Model 3

Figure 7. Phenomena of shear stress gradation in models with pull angles 85^0

Table 4. Shear stress on each towing lug models

No.	Pull Angle Variations (º)	τ (N/mm²)			τ allowable (N/mm²)	(τ) < (τ allowable)		
		Model 1	Model 2	Model 3		Model 1	Model 2	Model 3
1	80	80.09	100.91	103.84	138.89	pass	pass	pass
2	83	72.34	93.11	94.97	138.89	pass	pass	pass
3	85	66.90	87.43	88.65	138.89	pass	pass	pass
4	87	61.31	81.45	82.08	138.89	pass	pass	pass
5	90	54.46	72.10	71.95	138.89	pass	pass	pass

The subsequent shear stress is evaluated with the BKI class allowable shear stress. Where, from the 3 simulated models, all stress values meet the class criteria. The description of the comparison of the stress values for each model can be seen in the graph in Figure 8. In general, in terms of shear stress, all models and angle variations can be applied to the barge. However, it still needs to be considered on other types of working stress. Of the 3 simulated models, it seems that model 1 has a small shear stress value compared to models 2 and 3. In model 1, the doubling plate that is installed affects the decrease in the shear stress value. The increase in the value of the cross-sectional width (b) caused by the doubling plate also affects the increase in the inertia value of the pad eye. While the decrease in the trend of tension in each model is influenced by the sin direction of the tensile force acting on the towing lug.

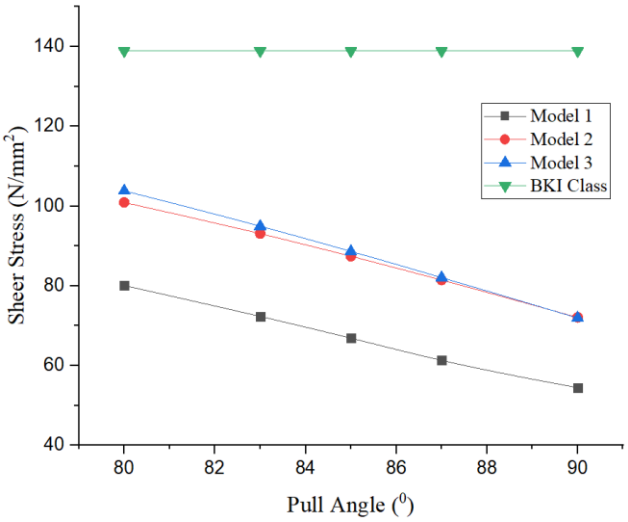

Figure 8. Shear stress distribution on towing lug models

3.3 Von Mises Stress

After obtaining the normal stress and shear stress values, the Von Mises stress on the towing lug structure is evaluated according to the class rules for each model as shown in Figure 9. The minimum Von Mises stress in model 1 is obtained at a pull angle of 90⁰. Meanwhile, the maximum Von Mises stress value in model 1 was obtained at a pull angle of 80⁰. The average percentage value of the stress drop for each change in the angle of model 1 is -4.81%. Furthermore, for model 2, the minimum Von Mises stress occurs at a pull angle of 90⁰ and the maximum Von Mises stress occurs at an angle of 80⁰. The average percentage value of the stress drop for each angle change in model 2 is -5.09%. The same phenomenon also occurs in model 3, where the minimum Von Mises stress value occurs at a pull angle of 90⁰ and the maximum Von Mises stress occurs at a pull angle of 80⁰. The average percentage value of the stress drop for each angle change in model 3 is -5.23%. The distribution of Von Mises stress values for each model can be seen in Table 5.

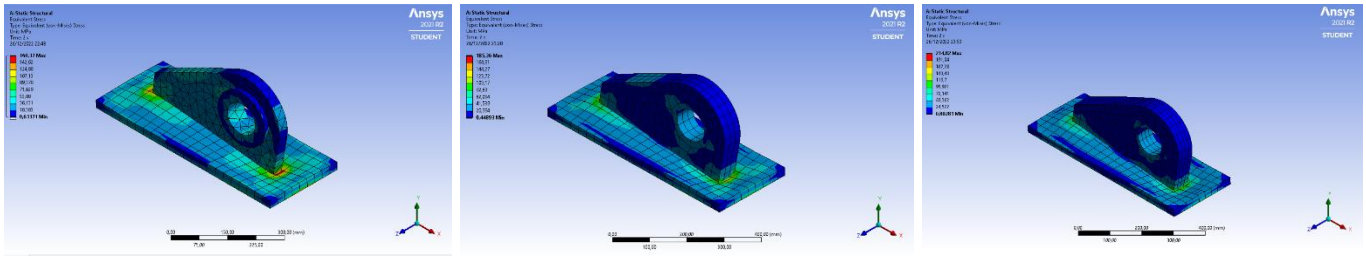

Model 1 Model 2 Model 3

Figure 9. Phenomenon of von mises stress gradation on models with pull angle of 90⁰

Table 5. Von mises stress on each towing lug models

No.	Pull Angle Variations (º)	σ_V (N/mm²)			$\sigma_{V\ allowable}$ (N/mm²)	$(\sigma_V) < (\sigma V_{\ allowable})$		
		Model 1	Model 2	Model 3		Model 1	Model 2	Model 3
1	80	195.36	228.51	266.38	250	pass	pass	fail
2	83	185.61	216.22	251.68	250	pass	pass	fail
3	85	178.66	207.71	241.50	250	pass	pass	pass
4	87	171.48	198.94	231.03	250	pass	pass	pass
5	90	160.37	185.36	214.82	250	pass	pass	pass

The Von Mises stress that occurs is then evaluated with the allowable von Mises stress of the BKI class. Where, from the 3 simulated models, 2 pull angles were obtained which did not match the BKI class allowable stress criteria as shown in Table 3. The description of the comparison of the stress values for each model can be seen in the graph in Figure 10. From the simulation results, the recommended pull angle on the withdrawal of the 300 feet barge, is vulnerable to 85^0-90^0. However, all variations can still be applied because all working stresses are still below the yielding stress of the towing lug material. For two points the von Mises stress which is above the allowable stress occurs because the difference between the working stresses in each direction (x, y, and z) is too large. This difference occurs because the line of action of the force is too dominant in only one force direction, in this case the x direction.

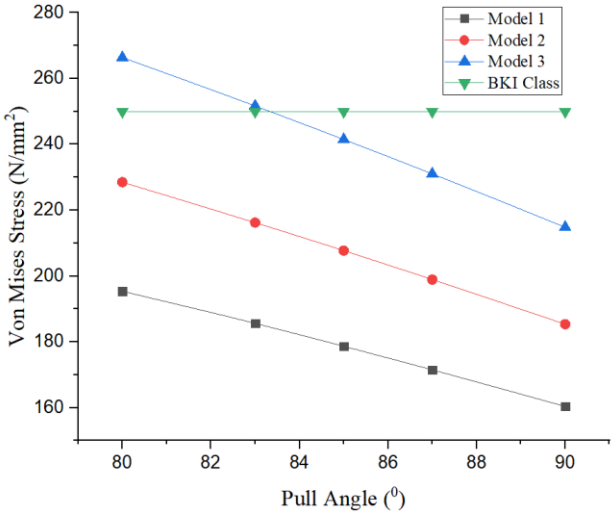

Figure 10. Von mises stress distribution on towing bracket

3.4 Deformation

In addition to the stress value, the maximum deformation number is considered in this simulation. For details of the maximum deformation values that occur in each simulation can be seen in Table 6. Overall, the deformations that occur are small because they are under 1 mm. In addition, the maximum deformation status that occurs is still in the elastic zone, allowing changes in the shape of the towing Lug structure to return to its original shape. For the deformation trend on the towing Lugat each tension angle the lowest occurs in model 3. Meanwhile, the deformation trend on the towing Lugat each maximum pull angle occurs in model 1 as shown in Figure 11. From the deformation trend in each model, it can be seen that the level of comparison of deformation numbers is a small one. The difference in deformation that occurs at each angle is caused by the asymmetric shape of the towing bracket. thus, the shape of the cross-section changes according to the direction of the force load. In general, all models of towing brackets are applicable when towing barges ashore.

Table 6. Deformation number on all models

Pull Angle Variation (^{0})	δ (mm)		
	Model 1	Model 2	Model 3
80	0.269	0.198	0.195
83	0.259	0.190	0.187
85	0.252	0.184	0.182
87	0.245	0.179	0.176
90	0.234	0.170	0.168

In the graph in Figure 11, Model 1 shows a very high deformation value when compared to the other 2 models. This is caused by the thickness of the pad eye connected to the main plate in model 1 is smaller than in models 2 and 3. Meanwhile, the trend of decreasing deformation values for each model is influenced by the value of the working load. Each inclination of the load on pull angle (Θ) of the pad eye causes a different force resultant. For this case the resultant force on the three models decreases at an angle range of 80^0 to 90^0.

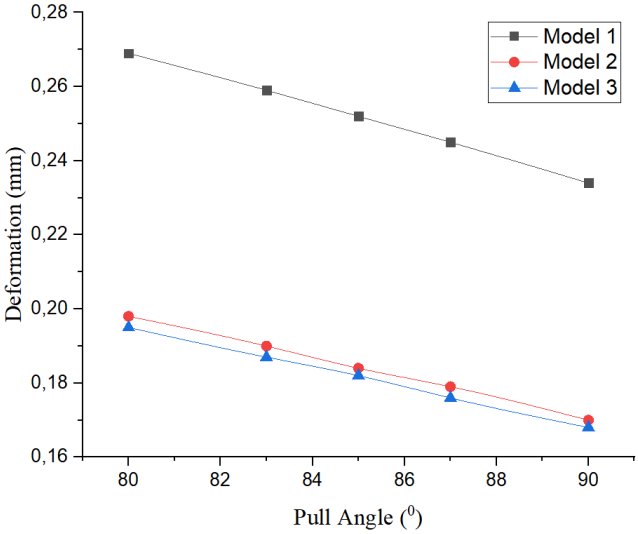

Figure 11. Maximal deformation ploting each models

4. Conclusion

The application of the computer-based finite element method (FEM) has been successfully carried out in this paper. The 3 models show varying strength values. Likewise, variations in the pull angle also show the same trend. In general, the strength of all towing bracket models is still quite good, where the working stress that occurs is still below the yield stress of the material. So that the deformation that occurs when the 300 feet barge is pulled is still in an elastic condition. In general, the equivalent stress in models 1, 2, and 3 experiences a decrease in value if the pull angle is enlarged. The percentage of settlement rate in each model starts from 4.81% for model 1, 5.09% for model 2, and 5.23% for model 3. Especially in model 3, two pull angle simulations produce equivalent stresses that exceed BKI's permitted equivalent stress. As a recommendation, the pad eye should be provided with a reinforcing structure such as a bracket to reduce the working stress.

References

[1] L. Wang, S. Li, J. Liu, Q. Wu, and R. R. Negenborn, "Ship docking and undocking control with adaptive-mutation beetle swarm prediction algorithm," *Ocean Engineering*, vol. 251, 2020, p. 111021, 2022, doi: 10.1016/j.oceaneng.2022.111021.

[2] G. M. Filho, P. I. D. Lameira, R. dos S. Saavedra, T. C. G. M. Filgueiras, and L. C. P. C. Filho, "Comparative study for naval repairs using longitudinal slipway or airbags," *Acta Scientiarum. Technology*, vol. 43, no. 2009, 2021, doi: 10.4025/ACTASCITECHNOL.V43I1.51796.

[3] M. Okereke and S. Keates, Finite Element Applications A Practical Guide to the FEM Process. 2018. doi: 10.1007/978-3-319-67125-3.

[4] C. Ranganayakulu and K. . Seetharamu, Compact Heat Exchangers – Analysis, Design and Optimization using FEM and CFD Approach. 2018.

[5] R. Kindmann and M. Kraus. Steel Structures: Design using FEM. Wilhelm Ernst & Sohn, Verlag fr Architektur und technische Wissenschaften GmbH & Co. KG, 2012. doi: 10.1002/9783433600771.

[6] N.-H. Heo and J.-S. Lee, "The Structural Strength Assesment of Lifting Lug," *Journal of the Society of Naval Architects of Korea*, vol. 51, no. 1, pp. 42–50, 2014, doi: 10.3744/snak.2014.51.1.42.

[7] J.-S. Lee and M.-S. Kim, "Ultimate Strength Assessment and Design of T type Lifting Lug," *ournal of the Society of Naval Architects of Korea*, vol. 52, no. 6, pp. 444–451, 2015, doi: 10.3744/snak.2015.52.6.444.

[8] J.-S. Lee and M.-S. Kim, "Strength Assessment of T-type Lifting Lugs Considering Deformation of Blocks," *Journal of Ocean Engineering and Technology*, vol. 29, no. 4, pp. 309–316, 2015, doi: 10.5574/ksoe.2015.29.4.309.

[9] Z. C. Liu, B. Zhou, and S. K. Tan, "Finite element analysis and structure optimum design of lifting padeye," *Advanced Materials Research*, vol. 658, pp. 399–403, 2013, doi: 10.4028/www.scientific.net/AMR.658.399.

[10] A. M. N. Arifuddin and Muhammad Uswah Pawara, "The Influence of Padeye Placement on Ship Block Lifting," *Majalah Ilmiah Pengkajian Industri*, vol. 16, no. 2, pp. 53–61, 2022, doi: 10.29122/mipi.v16i2.5255.

[11] L. P. Antalffy, G. A. Miller, K. D. Kirkpatrick, A. Rajguru, and Y. Zhu, "The design of lifting attachments for the erection of large diameter and heavy wall pressure vessels," *International Journal of Pressure Vessels and Piping*, vol. 139–140, pp. 12–21, 2016, doi: 10.1016/j.ijpvp.2016.02.020.

[12] F. Lv, X. Hu, C. Ma, B. Yang, and Y. Luo, "Failure analysis on cracking of backing plate of lifting lug for air preheater," *Engineering Failure Analysis*, vol. 109, no. January, p. 104395, 2020, doi: 10.1016/j.engfailanal.2020.104395.
[13] Biro Klasifikasi Indonesia, "Rules For Materials Consolidated Edition 2021," vol. V, Sec. 4, 2021.
[14] G. Sitepu, Hamzah, and L. O. A. R. Firu, "Study of the Use of Airbags System Dock Facilities at PT.Dock and Shipping Kodja Bahari Shipyaed II, Jakarta," pp. 181–192, 2012.
[15] BKI, "Consolidated Edition 2021," BKI Rules Hull Vol. II Tahun 2021, vol. II, 2021.